

STRESS INDUCED RELEASE OF Rn^{222} AND CH_4
TO PERCOLATING WATER IN GRANITIC ROCK

C. G. Sammis, M. Banerdt, and D. E. Hammond

Department of Geological Sciences
University of Southern California
Los Angeles, California 90007

Abstract The radon, methane, and carbon dioxide concentrations have been measured in water which has percolated through granitic rock under triaxial stresses ranging from 0.1 to 0.95 of the fracture stress. We simultaneously measured the permeability and porosity (hence hydraulic radius) of each sample. The first series of experiments were on seventeen initially dry rock samples. The radon concentration in the first 3 gm of water collected varied by a factor of 10, but was not correlated with stress. A good correlation was found between radon and permeability; rocks having high permeabilities tend to release less radon. In a second series of experiments, rock samples were saturated under stress, equilibrated for one month, then restressed and measured. These samples produced between 2 and 10 times more radon than initially dry rocks having the same permeability. In a third series of experiments, multiple successive water fractions were sampled. We found that most of the radon is removed with the first pore volume collected, while methane extraction requires several pore volumes. An experiment in which the stress was changed during a run produced an increase in CH_4 but no increase in Rn^{222} . These results are interpreted in terms of a numerical model for flow and gas extraction from a microcrack network.

Introduction The physical properties of radon gas (Rn^{222}) make it an ideal natural tracer for detecting changes in the fracture networks which permeate natural rock masses. As an intermediate daughter in the U^{238} decay series, Rn^{222} is constantly being generated in uranium bearing rocks. Formed by alpha-decay of the radium (Ra^{226}) parent, the radon atom has a recoil energy of about 100 KeV; sufficient energy to travel hundreds of lattice spacings upon formation. While most of these atoms lodge within the interior of a grain, some end up in the network of microcracks (and macrocracks) which permeate a rock mass, and may thereby enter the groundwater. The amount of radon dissolved in groundwater is thus primarily a function of the concentration and spatial distribution of radium within the rock, and the porosity and permeability of the fracture network. Changes in the fracture network

may change the ground water radon concentrations observed at a sampling site in two ways; (1) directly, by changing the number of radon atoms which enter the groundwater, and (2) indirectly by changing the transport of radon from the site at which it is created to the sampling site.

The relatively short half-life of Rn^{222} ($T_{1/2} = 3.825$ days) assures a short term causal relationship between changes in the fracture-network morphology and the resultant variation in groundwater radon. Because radon is an inert gas, it does not readily enter into chemical combination and its high solubility in water (22.4 cm^3 per 100 $\text{cm}^3 \text{H}_2\text{O}$ at 25°C and one atmosphere) means that, in the presence of groundwater, most radon will be dissolved rather than adsorbed to the walls of the fracture network. The physical mechanisms by which radon is generated and transported are discussed in more detail by Tanner (1980).

Two applications in which groundwater radon has been monitored are earthquake prediction and geothermal reservoir engineering. The build-up of tectonic stress preceding an earthquake might be expected to change the morphology of a fracture network by creating and opening cracks parallel to the maximum principal stress while closing orthogonal cracks. In the laboratory, the crack opening process dominates when the differential stress, $\sigma_1 - \sigma_3$ is greater than approximately one-half of the fracture stress and the rock actually increases in volume. Laboratory studies of this "dilatancy" phenomenon are reviewed by Brace (1978) and Byerlee (1978). Field observations of groundwater radon variations associated with earthquakes are summarized by Hauksson (1981) and Teng (1980). The withdrawal of water and heat from a geothermal reservoir might also be expected to change the morphology of the fracture network through the combined effects of thermal contraction and variations in pore pressure. The associated change in radon concentration could serve as a useful tool for monitoring reservoir development. Radon measurements in geothermal systems are discussed by Stoker and Kruger (1975).

Interpretation of field anomalies requires three basic sets of information: (1) a thorough understanding of the subsurface hydrology (reservoirs, permeabilities, and pressures), (2) a detailed knowledge of the subsurface geology (rock types and uranium concentrations), and (3) empirical relationships between changes in stress, the resulting changes in fracture permeability, and the associated release of radon (and other gases) into the groundwater (as a function of rock-type). The laboratory measurements reported below were designed to explore relationships required in step (3) above. We have focused on the relationships between differential stress, permeability, and the release of radon and methane to water percolating through the natural fracture network in granitic rock.

Previous Laboratory Studies of Radon Emanation and Transport There have been several laboratory studies of radon emanation from rock surfaces. Chiang et al. (1978) demonstrated that radon emanation is proportional to surface area by measuring the radon emanated from a number of rock samples having the same volume but different surface areas. The relation between stress and radon emanation has been studied by the Group of Hydrochemistry of the Peking Seismological Brigade (1977), Holub and Brady (1981), and Jiang and Li (1981). In each of these experiments, air was circulated around the rock sample (or through holes bored in the sample in the 1977 study) and uniaxial stress was applied. Radon levels in this circulating air were continuously monitored. In the two Chinese experiments only small increases in radon were observed during the uniaxial loading. Holub and Brady (1981) observed a large (50%) temporary increase in radon at about half the breaking strength of the sample, presumably due to the opening of axial microfractures at the onset of dilatancy. In all three experiments, the radon level increased by a factor between two and ten upon failure, probably reflecting the large increase in surface area directly accessible to the circulating gas.

The fundamental difference between these studies and our experimental work described below is that the above studies measured radon emanation from the surface of rock samples while we measured the radon released to water percolating through the microfracture system. We are thus able to look for quantitative correlations between radon release and stress, permeability, porosity, hydraulic radius, and crack surface area.

Experimental Apparatus The experimental apparatus is shown schematically in Figure 1 below. The triaxial pressure vessel is standard except for an outlet at the base to allow sampling of the pore water.

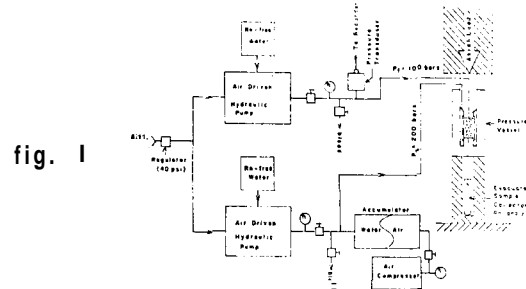


fig. 1

A cylindrical granite sample (two inches in diameter by four inches long) is loaded in the triaxial cell which is placed between the anvils of a 160,000 pound hydraulic press. This uniaxial stress is sufficient to cause failure of the samples under our nominal 200 bar confining pressure.

Confining pressure, σ_3 , and flow pressure, p_f , are generated by air-driven hydraulic pumps with special stainless steel valve isolation chambers to maintain water purity. Radon free distilled water is flowed through the sample at constant flow pressure p_f of 100 bars. A one millimeter thick layer of 200 mesh ZrC powder spreads the water at p_f over the entire top surface area, A , of the sample. The lower surface of the sample is maintained at $p=0$ since we are sampling into a vacuum. The base-plate has a pattern of radial and circumferential grooves which channel the flow water into the collection outlet hole. By measuring the amount of water as a function of time, the flow rate, $q(\text{cm}^3/\text{sec})$, is determined. Darcy's law may then be used to calculate the sample permeability, $k(\text{cm}^2)$, according to

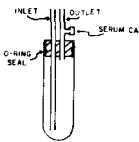
$$k = -q\mu l/Ap_f \quad (1)$$

where l is the sample length in cm and μ is the water viscosity in dynes sec/cm². We have been working at low values of the confining pressure (σ_3 nominally 200 bars). The functions of the confining pressure are (1) to seal the rubber sample jacket thus confining the fracture fluid within the sample, and (2) to maintain sample integrity at high values of uniaxial stress.

Granite Samples Approximately twenty feet of granite core was supplied by the U.S.G.S. The core is from the depth range 425-445 feet in the Sierra Nevada batholith, is very fresh, and appears both compositionally and mechanically uniform over its entire length. Radioactive analysis of six samples (chosen as representing extremes in observed radon production as discussed below) showed U^{238} concentrations between 2.50 and 3.10 ppm. Uranium concentration was uncorrelated with Rn^{222} concentrations observed in the percolating water.

Rn²²² Measurement Techniques Water samples were collected in evacuated pyrex test-tubes sketched below. Typical water samples were between 2 and 10 ml.

fig. 2



Radon was extracted from the water using recirculating helium as a carrier (e.g. Key et al., 1979). Radon was separated from the He carrier by two stages of liquid nitrogen cold-trapping. A drying column (CaSO₄+Ascarite) was used to separate CO₂ and H₂O from Rn²²² which was subsequently transferred to a scintillation cell. Radon gas levels were measured by counting scintillations associated with its α decay. The overall detection efficiency is about 80% as established by analyzing Ra²²⁶ standard solutions. The background level is 0.7 cpm (counts per minute)*; our experimental measurements are always at least a factor of four above this limit. Note that radon dpm (disintegrations per minute) reported below are less than the total observed cpm since the two alpha emitting daughters of Rn²²² (Po²¹⁸ and Po²¹⁴) are detected with the same efficiency as their parent.

CH₄ and CO₂ Measurement Techniques Before radon was extracted from some water samples, small (~ 1 cc) aliquots of the gas phase in the sample container were drawn into glass syringes through a rubber septum. These samples were injected into a gas chromatograph equipped with flame ionization and thermal conductivity detectors. CH₄ was isolated from other gases on a molecular sieve #5A column and CO₂ was isolated on a silica gel column. This sampling technique resulted in contamination of the sample with air, and typically 50-70% of the CH₄ and CO₂ peaks observed were due to this contamination. However, clearly detectable amounts of these two gases were released in most experiments. Analytical precision for duplicate analyses was about 8%. Blanks were run on the water before it passed through the rock to ensure that this was not a significant source of contamination. The total quantity of gas released from each sample was calculated by assuming equilibrium exists between liquid and gas in the sample container, knowing the volume of the gas and liquid phases in the container, and correcting for contamination from air (which was estimated from the O₂ content).

Experimental Procedures and Results Two series of experiments were run: experiments on initially dry rocks where a single water sample was collected, and experiments on dry and initially saturated rocks where sequential water samples were collected. In this second

*1 Curie=2.2 x 10¹² cpm

series the concentration of CH₄ and CO₂ were measured in addition to Rn²²².

In the initial series of experiments, a dry rock was jacketed and stressed axially to σ_1 , under a confining pressure of σ_3 . An evacuated sample collection vessel was then attached to the collection port in the baseplate, and a flow pressure, p_f , was established at the upper end of the sample at time $t=0$. The time at which the first drop of water appeared at the baseplate, t_f , was recorded, as was the time, t_s , when the sample bottle was sealed and removed. As discussed above, $\Delta t = t_s - t_f$ and the total volume were used to find the sample permeability. We show below that t_f may be used to find the sample porosity once the permeability is known.

The sealed sample vessel was then attached directly to the radon extraction apparatus and the radon concentration determined as discussed above. Following the radon extraction, σ_1 was increased slowly (40 bars/min) and the fracture stress, σ_f , was recorded.

The results of this first series of experiments are plotted as open circles in Figures 3-5.

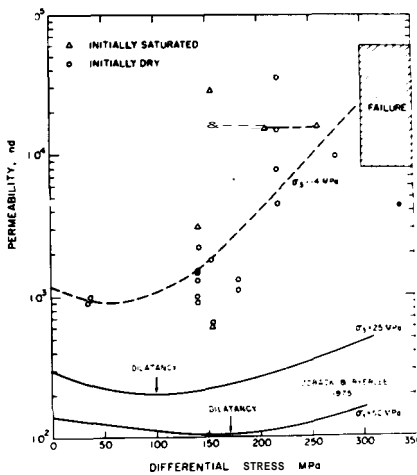


fig. 3

Figure 3 shows sample permeability, k , as a function of stress. Although the data scatter, they are consistent with a slight decrease in k with increasing σ_1 to approximately $\sigma_1 = \sigma_f/2$, followed by a more rapid increase in k as σ_1 approaches σ_f (as documented by Zoback and Byerlee (1975) at higher confining pressures). Our scatter is due to the fact that each data point represents a different rock, whereas Zoback and Byerlee measured k as a function of σ_1 on one sample. Figure 4 shows radon concentration in the first three grams of water collected as a function of the differential stress, $\sigma_1 - \sigma_3$. Note that there is no obvious relation between stress and radon. If the radon concentration is plotted as a function of the differential stress normalized to the fracture stress, $(\sigma_1 - \sigma_3)/\sigma_f$, there is still no obvious correlation.

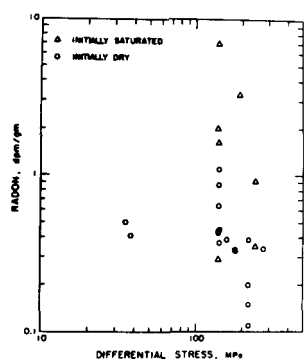


fig. 4

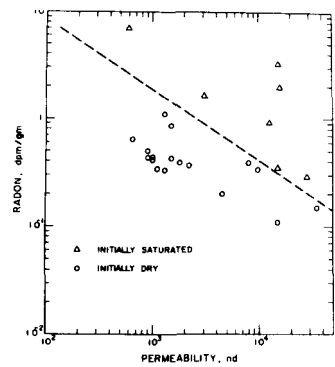


fig. 5

Figure 5 shows that radon concentration tends to decrease with increasing permeability.

The second set of experiments were designed to see if saturated rocks yield more radon than those which are initially dry. Several rock samples were stressed and saturated as above until the first drop of water was observed. They were then removed from the apparatus and stored under water for approximately one month to allow radon to establish an equilibrium concentration. They were then restressed and several successive water samples were collected. Sequential sampling experiments were also performed on two initially dry rocks for comparison.

The radon concentrations measured in the first three grams of water collected during these runs are plotted as open triangles in Figures 3-5. In Figure 5 it is apparent that, at a given permeability, the presence of water in the fracture network increases the radon release by a factor between two and ten.

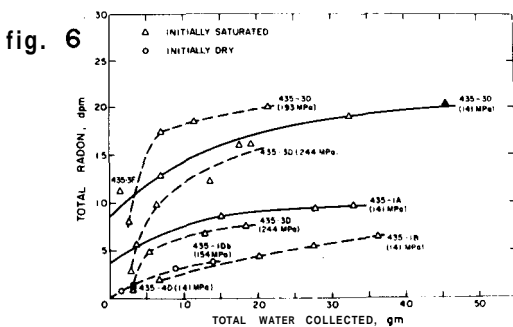


fig. 6

The results of the sequential sampling experiments are given in Figures 6 and 7 for radon and Figure 8 for nethane.

In Figure 6, the total radon is plotted as a function of the total water collected. The solid curves are calculated from a crack model discussed below. The dashed curves are sketched through data sets which could not be fit to the model.

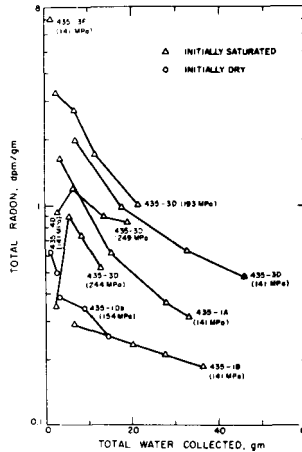


fig. 7

Figure 7 shows the radon concentration which would be measured if the experiment were stopped after the total amount of water shown on the abscissa had been collected.

Note that four of these multiple sample runs were on the same rock (435-3D). This rock was initially saturated, equilibrated, and then restressed to a differential stress of 141 MPa. Three successive water samples were collected. The stress was then increased to 193 MPa and a fourth sample was collected. This fourth point, the solid triangle in Figures 6 and 7, is on trend with the previous three points and shows no significant increase in radon following the stress change. The rock was then removed from the apparatus, re-equilibrated under water, and restressed to 193 MPa. The four, sequential, water samples collected at this stress contained slightly more radon (much less than a factor of two) than the 141 MPa run. The rock was removed, re-equilibrated, and then stressed to 244 MPa. Four samples were again taken, but this time an unusually low radon concentration was measured. The sample was observed to have developed a through-going, extensive fracture zone. Because the low radon level for this run is due almost entirely to the low concentration in the first sample collected, the rock was re-equilibrated and rerun at 244 MPa as a check. Again, the radon concentration in the first sample was anomalously low when compared with the other multiple sample runs.

In Figure 8, the total methane released is plotted as a function of the total water collected.

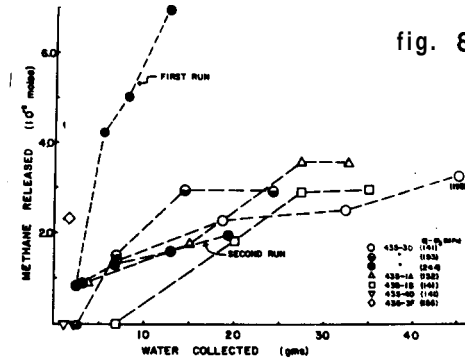


fig. 8

Note that the general shape of these curves is similar to the radon curves in Figure 6, but there are significant differences. More total water flow was required to extract all the available CH_4 ; in fact, some rocks released almost no methane to the first few grams of flow water. Also, the rock which was run at three different stresses (435-3D) released more methane at higher stresses. Even the stress change from 141 MPa to 193 MPa during the first run produced an increase in CH_4 concentration, while the Rn^{222} concentration was unaffected.

Carbon dioxide was more erratic than methane or radon when plotted as a function of total water collected. There was no apparent correlation between CH_4 , CO_2 , and Rn^{222} . Our interpretation of these results is that each of these gases must occupy different positions in the rock.

Sample Porosity and Hydraulic Radius The porosity of the sample under stress may be calculated from t_f , the time it takes to fill the initially dry rock with water. Following Brace et al. (1968) we approximate the flow law as $d^2p/dx^2 = 0$. Hence $dp/dx = f(t)$, i.e. the pressure gradient is approximated by a linear gradient which changes with time. Brace et al. (1968) have shown that transients due to \approx neglected terms are on the order of 10-30 sec. Since it takes at least an hour for our samples to fill, the linear gradient should be a good first approximation.

As water is pumped into the rock at a constant back-pressure, p_f , the water front will advance in the axial z direction at a rate

$$dz/dt = q/\eta A \quad (2)$$

where η is the porosity. Using Darcy's law (1) for q gives

$$dz/dt = -kp_f/\mu n z \quad (3)$$

which may be integrated to yield

$$\eta = 2kp_f t_f / \mu l^2 \quad (4)$$

Once the porosity and permeability are known, the hydraulic radius, m , may be found (m is defined as the volume of the cracks divided by their surface area). For intact rock, Brace (1978) gives

$$k = m^2 n^3 / k_0 \quad (5)$$

where k_0 is a geometrical factor between 2 and 3, while for dilatant microcracks in low porosity rock, permeability in the direction of the microcracks has the form

$$k = m^2 n / k_0 \quad (6)$$

For our samples the above analysis yielded porosities in the range 0.2% to 10%. Plotting porosity as a function of permeability yields k proportional to n^2 , between the n^3 dependence of (5) and the linear dependence of (6). The implication is that the microcrack orientations are somewhere between random and vertical. The observed radon release did not correlate with pore volume, hydraulic radius, or crack surface area.

Models for Radon Release We consider two extreme-case models for the radon extraction process: (1) a well-mixed reservoir model, and (2) a pipe-flow model.

In the reservoir model, we assume that

$$dn_r/dt = -qn_r/V_c \quad (7)$$

where n_r is the number of accessible radon atoms in the rock and V_c is the crack volume. Using $q \equiv dV/dt$ and $n_r + n_w = N_0$, where N_0 is the total accessible radon and n_w is the number of accessible radon atoms in the flow water, (2) may be rewritten and solved to give

$$n_w = N_0 [1 - \exp(-V/V_c)] \quad (8)$$

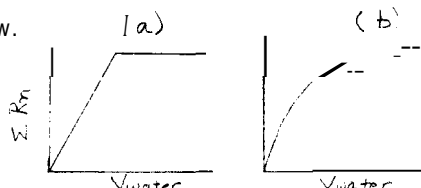
In terms of radon activity $a = \lambda n$ ($\lambda = 1.26 \times 10^{-4} \text{ min}^{-1}$)

$$a_w = A_0 [1 - \exp(1 - V/V_c)] \quad (9)$$

Only our dry samples, 435-4D and 435-1D could be fit to this model (solid lines in Figure 6). They both lie on the same curve which is defined by the parameters $A = 4.6 \text{ dpm}$ and $V = 9.0 \text{ cm}^3$. The total radon activity in these rocks should be $1.2 \times 10^3 \text{ dpm}$ (based on 3 ppm uranium). Hence we are removing about 0.4% of the available radon. A crack volume of 9 cm^3 corresponds to porosity (under stress) of about 4.5%, which seems a bit high.

None of the wet rocks could be fit to this model because the total radon curves in Figure 6 have too sharp a "knee" for the exponential form in (9). Such behavior is more typical of a pipe model which assumes all the radon is in solution and is simply pushed out by the advancing flow water with no mixing. In this case, Figures 6 and 7 should appear as sketched

below.



The initially saturated samples in Figure 6 look more like (a) above than the smooth curve predicted by (9). The true situation probably lies between these two extreme models, i.e. the water moves through as in a pipe model, but is continually being fed by side channels in the crack network thus rounding the sharp corners in (a) and (b) above.

Summary of Results We can briefly summarize our interpretation of the results presented in the previous section.

a. There was no correlation between radon released and stress applied to the initially dry samples. Among several possible explanations of this observation are: (1) the new microfractures opened by the higher stresses do not connect with the network of fractures which are carrying the water, and/or they do not carry a significant fraction of the water or (2) these new microfractures carry a significant fraction of the percolating water but they do not contain significant radon. They might not contain radon either because only pre-existing cracks have had time to concentrate and trap significant radon, or because radium is preferentially located as secondary surface coatings on existing cracks and this radium is responsible for virtually all of the observed Rn emanation (Tanner, 1980).

Explanation (1) is consistent with microscopic observations (Brace, 1977), but not with the results of the stress change experiment on sample 435-3D. The observation that Rn did not change while methane increased in response to a stress change during the first run on this sample implies that the flow water "saw" the new microcracks and removed the methane, but that there was no radon to be removed.

b. Samples which were saturated with water released more radon than those which were initially dry. These observations are not surprising in light of Tanner's (1980) discussion of the role of water as an absorber of the radon's recoil energy. Thus, the amount of water and the distribution of this water in the rock are critical factors controlling radon release.

c. Permeability and radon release are inversely correlated. This may be interpreted in two ways. Either water flows through the rock so quickly that radon does not have time to diffuse from side channels, or most of the water flows through a few, large, main channels (rather than many small channels) and thus removes a smaller fraction of the accessible radon atoms produced in the rock.

The hypothesis which is consistent with all our observations is that most of the observed radon is derived from radium which has been deposited on the walls of old microcracks. We are currently performing a series of experiments to test this hypothesis.

References

Brace, W. F., J. B. Walsh, and W. T. Frangos, "Permeability of granite under high pressure," *J. Geophys. Res.*, 73, 2225-2236.

Brace, W. F. (1977), "Permeability from resistivity and pore shape," *J. Geophys. Res.*, 82, 3343-13349.

Brace, W. F. (1978), "A note on permeability changes in geological material due to stress," *Pageoph.*, 116, 627-633.

Chiang, J. H., W. S. Moore, and P. Talwani (1977), "Laboratory studies of the relationship between surface area and radon release in Henderson gneiss," *Trans. Am. Geophys.*, 58, 434.

Hauksson, E. (1981), "Radon content of groundwater as an earthquake precursor: evaluation of worldwide data and physical basis," *J. Geophys. Res.*, 86, 9397-9410.

Holub, R. F., and B. T. Brady (1981), "The effect of stress on radon emanation from rock," *J. Geophys. Res.*, 86, 1776-1784.

Jiang, F., and G. Li (1981a), "The application of geochemical methods in earthquake prediction in China," *Geophys. Res. Letters*, 8, 469-472.

Key, R. M., R. L. Brewer, J. H. Stockwell, N. L. Guinasso Jr., and D. R. Schink (1979), "Some improved techniques for measuring radon and radium in marine sediments and in seawater," *Marine Chemistry*, 1, 251-264.

Stoker, A. K., and P. Kruger (1975), "Radon measurements in geothermal systems," Stanford Geothermal Program, Technical Report #4.

Tanner, A. B. (1980), "Radon migration in the ground: a supplementary review," *Natural Radiation Environment*, vol. 3, 5.

Teng, T. L. (1980), "Some recent studies on groundwater radon content as an earthquake precursor," *J. Geophys. Res.*, 85, 3089-3099.

The Group of Hydro-Chemistry, The Seismological Brigade of Peking (1977), "An experimental study of the relation between rock rupture and variation of radon content," *Acta Geophysica Sinica*, 20, No. 4, 277-282.

Zoback, M. D., and J. D. Byerlee (1975), "The effect of microcrack dilatancy on the permeability of westerly granite," *J. Geophys. Res.*, 80, 752.